Theoret. Chim. Acta (Berl.) 40, 323–341 (1975)

The Interaction of Alkali Metal Cations with Oxygen-Containing Ligands

Peter Schuster and Wolfgang Marius
Institut für Theoretische Chemie der Universität Wien

Alberte Pullman and Hélène Berthod
Institut de Biologie Physico-Chimique, Laboratoire de Biochimie Théorique
associé au C.N.R.S., Paris

Received September 9, 1975

Ab initio SCF calculations on the interaction of Li^+ cation with H_2O and H_2CO using two basis sets are presented. Partitioning of SCF energies of interaction into Coulomb-, exchange- and delocalization energies has been performed. Coulomb- and delocalization energies are compared with classical electrostatic and polarization energies. A detailed analysis of the calculated wave functions demonstrates that in the complexes investigated here, charge transfer is of minor importance only. Polarization of the molecules in the strong inhomogeneous field of the cation leads to complicated electron density rearrangements which can be interpreted most easily in terms of polarization of individual localized MO's.

Key words: Ion solvation – Ion-molecule complexes – SCF energy partitioning – Electrostatic energies – Molecular polarization

1. Introduction

During the last few years the interest in complexes between simple metal cations and molecules has increased tremendously. Many reasons are responsible for such a reinforced attention to this class of intermolecular associations. First of all, quantum mechanical calculations reached a stage of accuracy, which makes it possible nowadays to discuss structures and properties of this kind of complexes with a high degree of reliability. Starting off from extended basis sets the results of *ab initio* calculations provide material for discussions on safe grounds. On the other hand new experimental techniques were developed, e.g. high density mass spectrometry [1], which present the experimental basis for direct comparison of calculated and measured data. Furthermore a special class of compounds, ionophores or ion carriers, originally isolated from microorganisms as antibiotics, became a subject of central interest because of their high specificity in cation binding. Numerous model studies on transport of alkaline and alkaline earth ions through membranes by ionophores have been undertaken. In previous short communications [2, 3] we presented *ab initio* studies on the bond between Li^+ and oxygen-containing ligands. The present paper deals with the details of cation-molecule interactions and the nature of the metal ligand bond as far as they can

Table 1. Basis sets used in the SCF-calculations reported here

GTO's[a] Atom	Basis Set *A*	Basis Set *B*	Ref.
Li^+	7*s*, 1*p* (511, 1) [3*s*, 1*p*] $\xi_p = 0.1$	7*s*, 1*p* (511, 1) [3*s*, 1*p*] $\xi_p = 0.1$	[8]
H	4*s* (211) [3*s*]	4*s* (211) [3*s*]	[14]
C, O	9*s*, 5*p* (42111, 311 [5*s*, 3*p*]	9*s*, 5*p*, 1*d*[b] (42111, 311, 1) [5*s*, 3*p*, 1*d*] $\xi_d = 1.0$	[14]

[a] Cartesian Gaussian orbitals were used. Contractions are shown in brackets. The numbers of contractions finally applied in the variational procedure are given in square brackets. Orbital exponents and contraction coefficients were taken from the literature unless explicitly stated here.

[b] Only those *d*-orbitals which can participate in the occupied orbitals of H_2O or H_2CO were incorporated into the basis set: d_{zz}, d_{yz}, d_{zx}.

be derived from SCF energy partitioning [4–6] and from an analysis of the complexes' wave functions.

In order to keep computer time for numerical calculations within certain reasonable limits we had to restrict ourselves to the smallest metal cation possible, Li^+, as well as to small ligands, which can act as reasonable models for lone pair and π-electron donors, like the molecules H_2O and H_2CO. Consequently, we will describe here the results of a series of calculations on $Li^+...OH_2$ and $Li^+...OCH_2$ with different basis sets and analyse the wave functions of these complexes.

2. Method of Calculation

Starting from medium size basis sets with and without polarization functions for second row elements (Table 1) we performed *ab initio* calculations at the SCF-level on $Li^+...OH_2$ and $Li^+...OCH_2$. The computer program used was a version of IBMOL V [7] adapted especially for an IBM 370/165 computer (C.I.R.C.E., Orsay). In all our calculations the geometry of the molecule bound to the cation was kept constant. Bond lengths and bond angles used are summarized in Table 2. Some recent calculations have shown that this restriction does not cause serious errors as long as we consider the type of cation-molecule complexes we are interested in here: $Li^+...OH_2$[8, 24], $Li^+...NCH$ [9].

Table 2. Molecular geometries applied in the SCF calculations

Molecule	Geometry
H_2O	$R_{OH}=0.958$ Å, $\sphericalangle$ HOH $=104.5°$
H_2CO	C_{2v}-Symmetry $R_{CH}=1.12$ Å, $R_{CO}=1.21$ Å, $\sphericalangle$ HCH $=118°$

For our purpose, the geometry of the complex is described best by the following choice of coordinate system (see Fig. 1). The z-axis coincides with the axis of symmetry of the ligand. In both examples we are discussing here (H_2O and H_2CO) this is the C_2 axis. As the other two coordinates two angles, ω and $\theta(0\leqslant\omega<\pi,\ 0\leqslant\theta<2\pi)$ or two distances, x and y can be used equally to fix the cation within a given plane $z=z_{Li+}$. The molecular plane of the ligand is chosen to coincide with the xz-plane of our coordinate system.

Individual contributions to the SCF-energy of interaction were calculated by SCF energy partitioning according to Dreyfus and Pullman [4]. The following quantities were computed as energy expectation values by starting from appropriately defined wave functions of the complex:

1. The Coulomb energy of interaction, ΔE_{COU}

$$\Delta E_{COU}=\int\psi_1^*\hat{H}\psi_1 d\tau-(E_M^0+E_L^0);\quad \psi_1=\psi_M^0\cdot\psi_L^0 \tag{1}$$

Here and in the following equations ψ_M^0 and ψ_L^0 are antisymmetrized and normalized SCF wavefunctions of the isolated subsystems, the metal cation (M) and the ligand molecule (L). $\hat{H}$ is the complexes' full Hamiltonian and E_M^0 and E_L^0 finally represent the energies of the isolated subsystems M and L obtained simultaneously with ψ_M^0 and ψ_L^0 by independent SCF-calculations.

2. The total first order energy of interaction, $\Delta E(1)$

$$\Delta E(1)=\int\psi_2^*\hat{H}\psi_2 d\tau-(E_M^0+E_L^0);\quad \psi_2=\mathscr{A}\{\psi_M^0\cdot\psi_L^0\} \tag{2}$$

In contrast to ψ_1, ψ_2 is not a simple Hartree product but a normalized and antisymmetrized wave function of the complex. Analogously to the result of

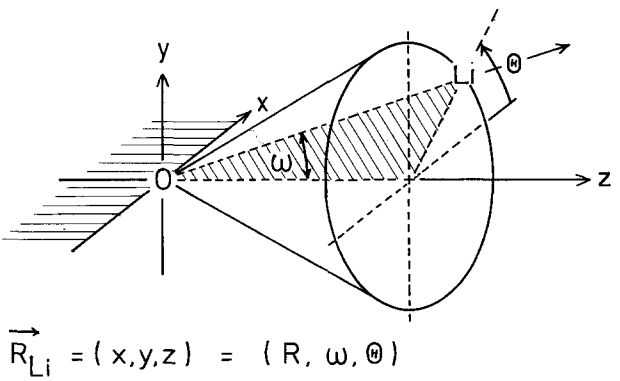

Fig. 1. Coordinate system defining the position of Li^+ cation relative to the ligand (z-axis $=C_2$ axis)

intermolecular perturbation theory $\Delta E(1)$ can be interpreted as a sum of a Coulomb and exchange contribution, $\Delta E_{COU} + \Delta E_{EX}$:

$$\Delta E_{EX} = \Delta E(1) - \Delta E_{COU} \tag{3}$$

3. The SCF energy of interaction ΔE:

$$\Delta E = \int \psi_3^* \hat{H} \psi_3 d\tau - (E_M^0 + E_L^0); \quad \psi_3 = \psi_{ML} \tag{4}$$

ψ_{ML} is the normalized and antisymmetrized wave function obtained by the full SCF calculation of the whole complex. Within the framework of SCF calculations there are two major second order contributions in a perturbational treatment of intermolecular energies: the polarization energy ΔE_{POL} and the charge transfer term ΔE_{CHT}. Dispersion interaction, ΔE_{DIS}, in molecular complexes can be described by certain doubly excited configurations only and consequently does not appear in the asymptotic SCF energy of interaction. From Eq.(4) we can obtain the two second order terms mixed together with higher order contributions as a measure of the energetical result of electron delocalisation, ΔE_{DEL}:

$$\Delta E_{DEL} = \Delta E - \Delta E(1) = \Delta E_{POL} + \Delta E_{CHT} + \Delta E(3) + \cdots \tag{5}$$

In the calculations reported here we analyse our total energy of interaction in terms of ΔE_{COU}, ΔE_{EX} and ΔE_{DEL}.

In order to learn more about the nature of the metal ligand interaction the SCF wave function of the complex was analysed in more detail. Mulliken overlap populations [10] give only a rough picture of the changes in electron densities due to the complex formation. Therefore we calculated also quantities derived directly from three dimensional one electron densities ρ by partial integration. An integrated density difference function of the complex ML, $\Delta\rho_{ML}(z)$, has been found to be appropriate for the kind of representation we desire here [2]:

$$\Delta\rho_{ML}(z) = \int\int [\rho_{ML}(\vec{r}) - \{\rho_M(\vec{r}) + \rho_L(\vec{r})\}] dx dy \tag{6}$$

A still more detailed information can be obtained in case the density difference function is calculated for different localized orbitals of the cation and the ligand separately (Figs. 2 and 3). The localization of the canonical orbitals was performed with a computer program using Ruedenberg's procedure [11]. The orbitals calculated by this procedure are fully localized: instead of σ and π-type functions we obtain equivalent "banana" bond orbitals.

Integrated density difference curves $\Delta\rho_{ML}(z)$ were found to be useful also for a definition of charge transfer between the subsystems forming a complex independent from population analysis. Provided a definition for the border between cation and ligand can be given charges are obtainable simply by integration. According to our model considerations the border is represented by a plane $z = z_0$:

$$Q_L = \int_{-\infty}^{z_0} \Delta\rho_{ML}\, dz \quad \text{and} \quad Q_M = \int_{z_0}^{\infty} \Delta\rho_{ML}\, dz \tag{7}$$

Charge transfer is represented now as the change in charge on complex formation:

$$\Delta Q_L = Q_1 - Q_L^0 = -\Delta Q_M = Q_M - Q_M^0 \tag{8}$$

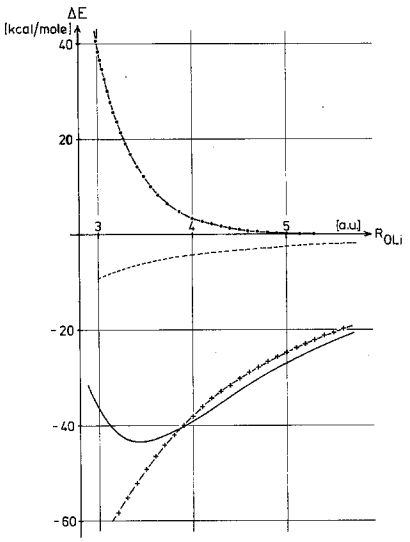

Fig. 2. Partitioning of total energy of interaction ΔE in $Li^+...OH_2$ into Coulomb-, exchange- and delocalization terms as a function of the ion ligand distance R_{OLi^+}.
ΔE:————; ΔE_{COU}:– + – + – + – ΔE_{EX}–·–·–·–; ΔE_{DEL}:– – – – (Basis set *A*)

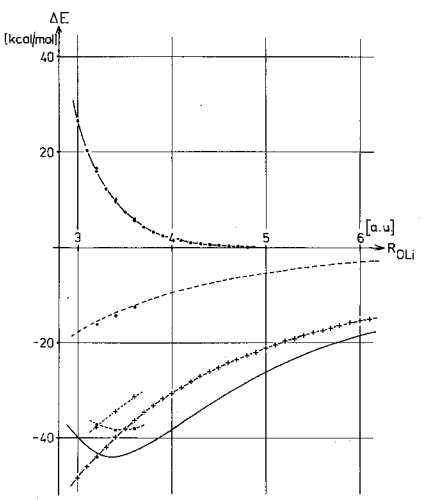

Fig. 3. Partitioning of total energy of interaction ΔE in $Li^+...OCH_2$ into Coulomb-, exchange- and delocalization terms as a function of the ion ligand distance R_{OLi^+}.
ΔE————; ΔE_{COU}:– + – + – + – ΔE_{EX}:–·–·–·– ΔE_{DEL}:– – – – (Basis set *A*)
ΔE: ––·––·––; ΔE_{COU}: ––+––+––+–; ΔE_{EX}:–·–·–·–; ΔE_{DEL}:· · · · (Basis set *B*)

Table 3. Electric properties of the isolated Li^+ cation and the ligand molecules

Molecule or Ion	Method[a]	Ref.	Multipole Moments $\mu_z(D)$	θ_{xx}[b]	θ_{yy}[b]	θ_{zz}[b]	Polarizabilities ($Å^3 = 10^{-24}$ cm^3)[c] α_{xx}	α_{yy}	α_{zz}	$\bar{\alpha}$
Li^+	SCF, A	—	—	—	—	—	0.026	0.026	0.026	0.026
	EXP	[19]	—	—	—	—	0.027	0.027	0.027	0.027
H_2O	SCF, A	—	−2.64	2.52	−2.33	−0.19	1.026	0.350	0.729	0.702
	SCF, B	—	−2.34	2.54	−2.45	−0.09	1.035	0.476	0.775	0.726
	SCF, C	[15, 16]	−2.00	2.53	−2.42	−0.11	1.071	0.589	0.749	0.803
							(1.651)	(1.226)	(1.452)	(1.443)
	SCF, D	[17]	−1.96				1.246	1.011	1.150	1.136
	EXP	[20–22]	−1.85±0.03	2.63±0.02	−2.50±0.02	−0.13±0.03				1.45
H_2CO	SCF, A	—	−3.02	0.55	0.05	−0.60	1.870	0.929	2.952	1.917
	SCF, B	—	−2.79	0.29	−0.07	−0.22	1.989	1.028	2.895	1.971
	SCF, C	[16, 18]	−2.82	0.25	−0.26	0.01	(2.170)	(2.313)	(4.553)	(3.292)
	EXP	[20, 23]	−2.33±0.02	−0.6±0.7		−0.75±0.8				

[a] Basis sets *A* and *B*: this paper (see Table 1); basis set *C*: GTO (10*s*, 6*p*, 2*d*/4*s*2*p*) and Basis set *D*: STO double zeta, polarization functions included.

[b] Center of mass was used as origin of the coordinate system; units: 10^{-26} esu·cm^2.

[c] Results from uncoupled Hartree-Fock pertubation theory are not comparable with those calculated from coupled Hartree-Fock equations and consequently given in parentheses.

Table 4. SCF-Energy partitioning in $Li^+ \ldots OH_2$

R_{OLi} a.u.	Å	Basis Set	Energies in kcal/mole ΔE_{COU}	$\Delta E^{(1)}$	ΔE_{EX}	ΔE	ΔE_{DEL}
3.0	1.588		−65.8	−27.7	38.1	−36.8	−9.1
3.2	1.693		−58.3	−34.3	24.0	−41.8	−7.5
3.4	1.799		−51.9	−36.9	15.0	−43.4	−6.5
3.6	1.905		−46.5	−37.2	9.3	−43.0	−5.8
4.0	2.117	*A*	−38.0	−34.5	3.4	−39.2	−4.6
4.4	2.328		−31.6	−30.4	1.2	−34.1	−3.8
4.8	2.540		−26.7	−26.3	0.4	−29.3	−3.0
5.4	2.856		−21.3	−21.2	0.1	−23.3	−2.1
3.4	1.799	*B*	−44.2	−29.3	14.9	−37.3	−7.9

Table 5. SCF-Energy partitioning in $Li^+ \ldots OCH_2$

R_{OLi} a.u.	Å	Basis Set	Energies in kcal/mole ΔE_{COU}	$\Delta E^{(1)}$	ΔE_{EX}	ΔE	ΔE_{DEL}
3.0	1.588		−48.7	−22.1	26.6	−39.9	−17.8
3.2	1.693		−43.4	−27.9	16.0	−43.4	−15.6
3.4	1.799		−39.8	−30.2	9.6	−44.0	−13.8
3.6	1.905		−36.3	−30.6	5.7	−42.9	−12.3
3.8	2.011		−33.2	−29.9	3.4	−40.8	−10.9
4.0	2.117	*A*	−30.6	−28.6	1.9	−38.3	− 9.7
4.2	2.223		−28.2	−27.1	1.1	−35.6	− 8.5
4.4	2.328		−26.1	−25.5	0.6	−33.0	− 7.6
4.8	2.540		−22.6	−22.4	0.17	−28.3	− 5.9
5.2	2.758		−19.7	−19.7	0.03	−24.3	− 4.6
5.6	2.963		−17.4	−17.4	—	−21.0	− 3.6
6.0	3.175		−15.4	−15.4	—	−18.3	− 2.9
7.0	3.704		−11.8	−11.8	—	−13.4	− 1.6
10.0	5.292		− 6.2	− 6.2	—	− 6.6	− 0.4
3.2	1.693		−37.7	−21.1	16.6	−37.3	−16.2
3.4	1.799	*B*	−34.4	−24.4	10.0	−38.5	−14.2
3.6	1.905		−31.4	−25.5	5.9	−38.0	−12.5

Three definitions of the separating plane $z=z_0$ have been used previously and were found to be equally satisfactory for a comparison of different complexes [12, 13]. Here we use the point of minimal integrated density, $\rho_{ML}(z)$, for this purpose:

$$\left(\frac{\partial \rho_{ML}}{\partial z}\right)_{z=z_0} = 0 \tag{9}$$

3. Results

In order to facilitate comparison with classical and semiclassical theories we calculated some electric properties of the isolated ligand molecules within the limitations of the basis sets applied here. The results obtained are compared with those of more accurate calculations and with experimental data in Table 3.

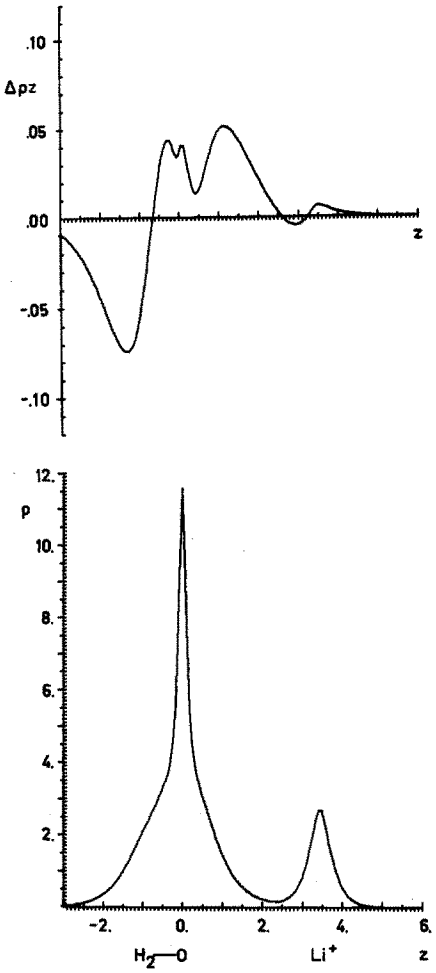

Fig. 4A. Total integrated density function ρ_z and integrated density difference function $\Delta\rho_z$ for $Li^+...OH_2$ (Basis set *A*)

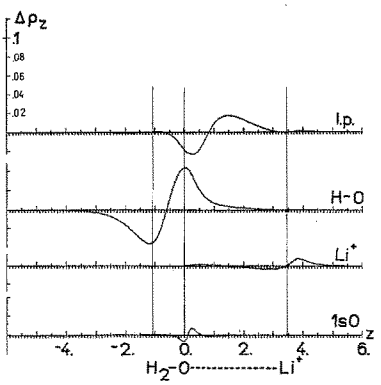

Fig. 4B. Decomposition of the integrated density difference function $\Delta\rho_z$ into contributions from individual localized MO's (a basis set similar to basis set *A* was used: (9*s*, 5*p*) [2*s*, 2*p*] on O, (4*s*) [2*s*] on H and (9*s*, 1*p*) on Li^+). Units: *z*-axis in [a.u.]'s, ρ_z and $\Delta\rho_z$ in units of [electrons/a.u.]

SCF energies and the results of energy partitioning are summarized in Tables 4 and 5 for $Li^+...OH_2$ and $Li^+...OCH_2$ respectively. As it is well known from previous calculations (cf. [13]) the energies obtained depend strongly on the basis set applied. Our example demonstrates the strong influence of polarization functions particularly on Coulomb energies.

Energy curves for complex formation on an approach of the cation along the *z*-axis are shown in Figs. 2 and 3. Although the curves for the total energies, $\Delta E(R_{OLi})$, are very similar in both cases studied here, energy partitioning shows substantial differences.

Density difference curves, $\Delta\rho_{ML}(z)$ are shown in Figs. 4 and 5 together with the corresponding curves for the total density $\rho(z)$ as well as with the contributions of individual orbitals. Partitioning of the overall changes into these contributions

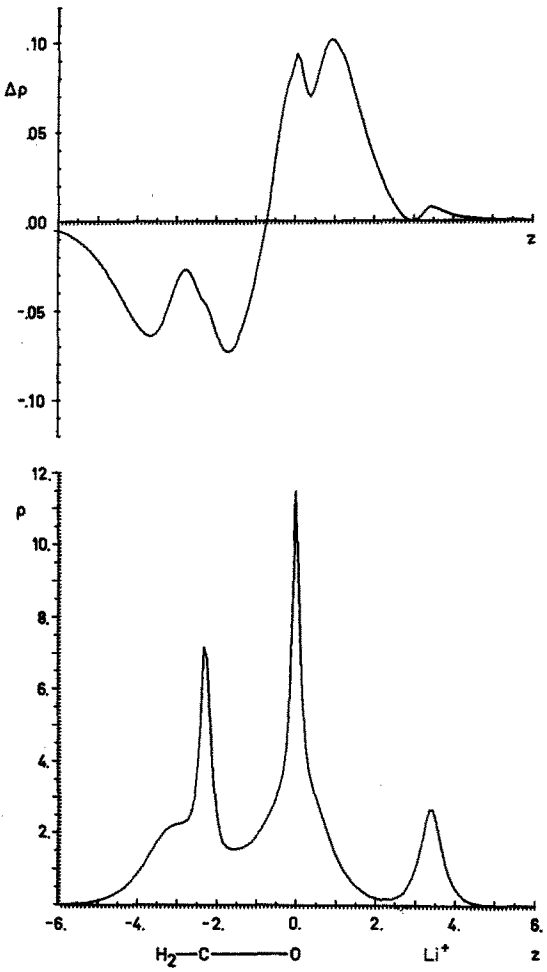

Fig. 5A. Total integrated density function ρ_z and integrated density difference function $\Delta\rho_z$ for $Li^+ \ldots OCH_2$ (Basis set *B*)

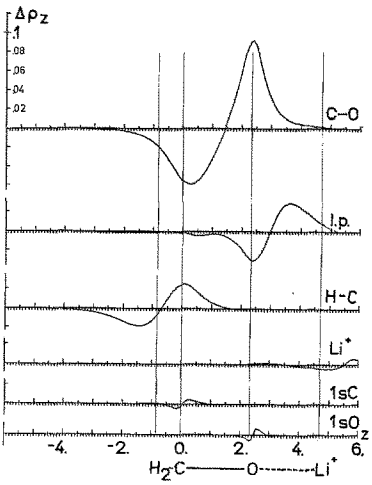

Fig. 5B. Decomposition of the integrated density difference function $\Delta\rho_z$ into contributions from individual localized MO's (a (5*s*, 3*p*) [3*s*, 2*p*] set of GTO's on O and C, (2*s*) on H and (9*s*, 1*p*) on Li^+ was used as basis). Units: *z*-axis in [a.u.]'s, ρ_z and $\Delta\rho_z$ in units of [electrons/a.u.]

is really illustrative and represents interesting information on the nature of the metal ligand interaction.

In order to be able to follow the increase in mutual polarization during an approach of the cation $\Delta\rho_{ML}(z)$ was calculated at different intermolecular distances R_{OLi}. The whole set of curves is shown in three dimensional plots $\Delta\rho_{ML}(z, R_{OLi})$ in Figs. 6 and 7 for the complexes under investigation here.

Finally, changes in atomic net charges were calculated by Mulliken population analysis (Table 6). They again reflect the strong polarizing effect of the cation. Charge transfer was investigated by both population analysis and integration of density difference curves as suggested in Eq.(8). The results are summarized in Table 7.

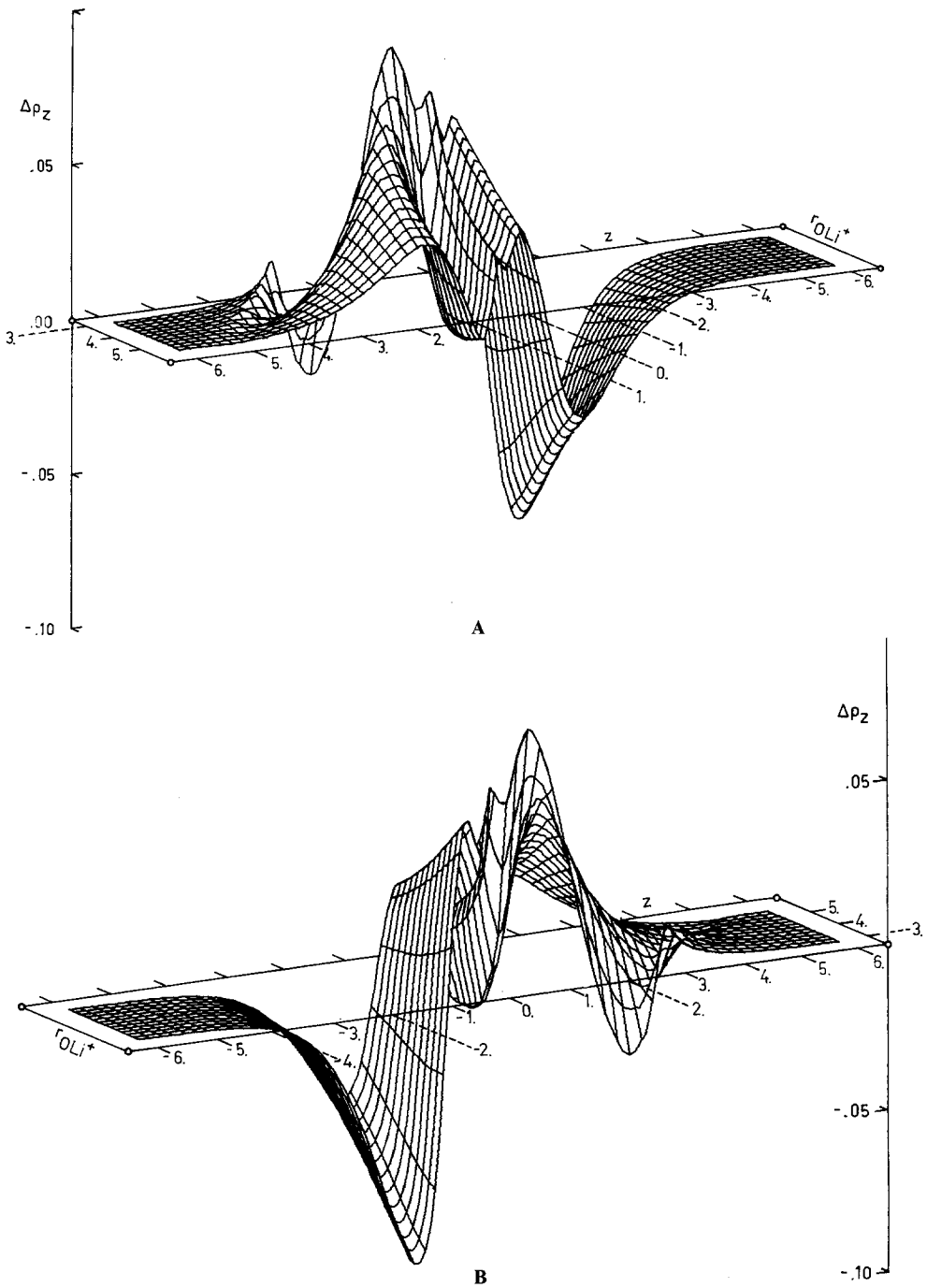

Fig. 6. Integrated density differences $\Delta\rho_z$ as functions of the ion ligand distance R_{OLi+} (Basis set *A*). A: seen in the direction of decreasing ion-ligand distance. B: seen in the direction of increasing ion-ligand distance. Units and positions of O and H are the same as in Fig. 4A

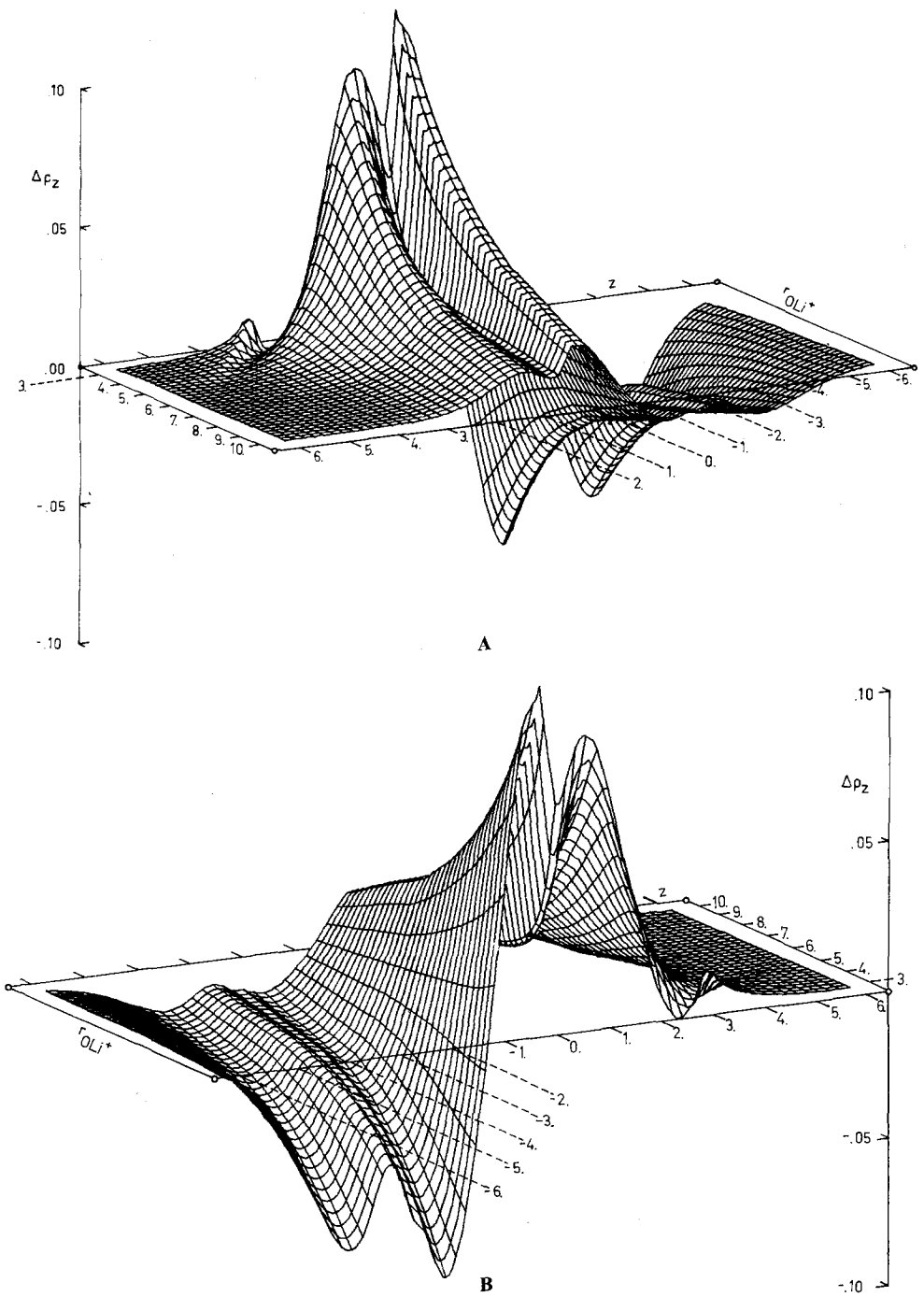

Fig. 7. Integrated density differences $\Delta\rho_z$ as functions of the ion-ligand distance R_{OLi^+} (Basis set *A*). A: seen in the direction of decreasing ion-ligand distance. B: seen in the direction of increasing ion-ligand distance. Units and positions of C, O and H are the same as in Fig. 5A

Table 6. Mulliken populations in $Li^+ \cdots OCH_2$: Net charges q

R_{OLi}		Basis Set *A*				Basis Set *B*			
a.u.	Å	q_H	q_C	q_O	q_{Li}	q_H	q_C	q_O	q_{Li}
3.2	1.693	0.230	0.251	−0.684	0.974				
3.4	1.799	0.225	0.237	−0.660	0.973	0.215	0.259	−0.671	0.973
3.6	1.905	0.221	0.226	−0.640	0.973				
4.0	2.117	0.212	0.209	−0.607	0.974				
4.4	2.328	0.204	0.196	−0.579	0.975				
∞	∞	0.137	0.117	−0.390	1.0	0.126	0.166	−0.418	1.0

Table 7. Charge transfer in Li^+ complexes

R_{OLi}		Charge Transfer, $\Delta Q(e_0)$[a]	
a.u.	Å	$Li^+ \ldots OH_2$	$Li^+ \ldots OCH_2$
3.0	1.588	−0.0099	
3.2	1.693		0.0126 (0.026)
3.4	1.799	0.0022	0.0127 (0.027)
3.6	1.905	0.0052	0.0129 (0.027)
4.0	2.117	0.0060	0.0091 (0.026)
4.4	2.328	0.0054	0.0064 (0.025)
4.8	2.540	0.0036	0.0043
5.2	2.752		0.0027
5.4	2.858	0.0018	
6.0	3.175		0.0009

[a] Values derived from Mulliken populations are shown in parentheses.

4. Discussion

In the present paper we restrict our discussion to an approach of the cation along the C_{2v} axis of the ligand molecule. Two main reasons justify this particular choice: electrostatic models and previous calculations [2, 3, 8, 24–26] have shown that the adiabatic path of complex formation in $Li^+ \ldots OH_2$ and $Li^+ \ldots OCH_2$ preserves C_{2v} symmetry indeed. Secondly, we are mainly concerned here with a comparison of complexes formed by two different ligand molecules of closely related symmetry properties and it seems reasonable to start out from those configurations which are completely determined by symmetry.

At the energy minima total energies for complex formation are roughly the same in both examples studied here. Furthermore, metal ligand distances (R_{OLi}) at equilibrium are very similar. The following values were calculated with basis set *A*:

$$Li^+ \ldots OH_2: R^0_{OLi} = 3.46 \text{ a.u.} = 1.83 \text{ Å}, \Delta E(R^0) = -43.5 \text{ kcal/mole}$$
$$Li^+ \ldots OCH_2: R^0_{Li} = 3.37 \text{ a.u.} = 1.78 \text{ Å}, \Delta E(R^0) = -44.0 \text{ kcal/mole}$$

Considering SCF energy partitioning, however, we can realize a substantial difference between the two cases. First of all, the electrostatic or Coulomb contribution predominates even more in $Li^+ \ldots OH_2$ than in $Li^+ \ldots OCH_2$. At the first

glance exchange energy is not too different in the two complexes. Consequently, the contribution of the electron delocalization is compensating for the difference in electrostatic energies and in fact ΔE_{DEL} is about twice as large in absolute value in $Li^+...OCH_2$ compared to the $Li^+...OH_2$ complex.

Concerning the results with basis set *B*, although only one type of polarization function has been added to basis set *A*, substantially different numbers are obtained with the enlarged basis:

$$Li^+...OCH_2: R^0_{OLi} = 3.44 \text{ a.u.} = 1.82 \text{ Å}, \Delta E(R^0) = -38.6 \text{ kcal/mole},$$

thus showing a decrease of 5.4 kcal/mole in the binding energy, together with a slight increase in the equilibrium distance. The energy decomposition (Table 5) indicates that this decrease in the binding energy is brought about essentially by the decrease in the Coulomb component which, however, remains the dominant term. Analogous trends appear in the case of H_2O (Table 4).

The decrease obtained in the Coulomb attraction parallels the decrease in the computed value of the dipole moment brought about by the introduction of the polarization functions (Table 3). One may expect that a further improvement of the wave function such as to reproduce the experimental multipole moments would further decrease the value of ΔE_{COU}. Unfortunately, as seen by the data in Table 3, a very good accuracy for these quantities is not realized by SCF computations even near the Hartree-Fock limit where the dipole moments for H_2O and H_2CO are still calculated substantially too large. A more accurate description of these properties of the isolated subsystems would require an explicit consideration of electron correlation. Since calculations of this degree of accuracy on the complexes as a whole are extremely time consuming, we decided to try an alternative approach. Most properties of isolated ions and ligands are often known either from reliable experiments or from very accurate calculations or even from both, and there is no reason not to make use of this information. Calculations with small basis sets will be used therefore as a starting point testing the applicability of simple classical expressions into which afterwards the correct molecular properties might be inserted. In this way also, the sensitivity of the energy partitioning to the extension of the basis set [28, 13] may be better understood and corrected [27, 29, 30].

The Coulomb energy, ΔE_{COU} should converge asymptotically to the expression of classical electrostatics at the limit of large intermolecular distance. For our purpose here it is important to have a good estimate of the errors introduced into the calculations on our concrete examples by partial overlap of the subsystem and by a single center expansion of molecular potentials. In classical electrostatics the interaction of an ion with a molecule along its *z*-axis can be described by the well-known power series of multipole moments which was extended here up to the second term only:

$$\Delta E^{\mathrm{SC}}_{\mathrm{COU}} = \frac{q}{R^2}\left(\mu_z + \frac{\theta_{zz}}{R}\right) + \cdots \tag{10}$$

In all calculations reported here the molecular center of mass (C.M.) was used as the origin of the coordinate system. A more systematic study on the influence of

Table 8. Coulomb energy of interaction obtained by SCF energy partitioning and classical electrostatic models[a]

	$Li^+\cdots OH_2$		$Li^+\cdots OCH_2$		
R_{OLi}(a.u.)	ΔE_{COU}	ΔE_{COU}^{SC}[b]	ΔE_{COU}	ΔE_{COU}^{MC}[b]	ΔE_{COU}^{SC}[a]
3.0	−65.75	−69.70	−48.65	−47.82	−47.42
3.2	−58.27	−61.41	−43.43		−42.98
			(−37.74)		(−37.28)
3.4	−51.92	−54.52	−39.82		−39.14
	(−44.2)	(−47.5)	(−34.36)		(−34.51)
3.5				−37.76	−37.41
3.6	−46.52	−48.72	−36.30		−35.79
			(−31.42)		(−31.62)
4.0	−37.95	−39.59	−30.56	−30.53	−30.27
4.4	−31.56	−32.81	−26.10		−25.93
4.5				−25.18	−24.99
4.8	−26.68	−27.63	−22.57		−22.46
5.0				−21.12	−20.98
5.2			−19.72		−19.64
5.4	−21.25	−21.89			
5.6			−17.39		−17.32
6.0			−15.43	−15.39	−15.47
7.0			−11.78	−11.81	−11.77
8.0				− 9.32	− 9.29
10.0			− 6.19	− 6.22	− 6.21

[a] All energies in kcal/mole calculated with basis set *A*; values obtained with basis set *B* are given in parentheses.

[b] ΔE_{COU}^{SC} and ΔE_{COU}^{MC} were calculated from classical electrostatic expressions; "SC" means single center, "MC" multiple center expansion up to quadrupole moments (see text).

the choice of the origin will be presented in a forthcoming paper [27]. In addition, the electrostatic potential of H_2CO was calculated by a multicenter expansion, which has been described previously [31, 32] and was used in various calculations of molecular properties. Our results are summarized in Table 8. Fairly good agreement between ΔE_{COU} and the results derived from Eq.(10) is found provided molecular properties calculated with the same basis set were inserted. In the case of $Li^+...H_2CO$ the agreement is somewhat better than in the water complex. Multicenter expansion of the potential does not modify the results substantially although it brings them slightly closer to the exact values at short distances. At large distances the expected asymptotic convergence of ΔE_{COU},ΔE_{COU}^{SC} and ΔE_{COU}^{MC} is found.

Polarization energies can be calculated easily from classical electrostatic formulas provided molecular polarizabilities are known. In complexes of Li^+ the polarizability of the cation is so small that only the polarization of the molecule in the field of the cation gives an important contribution to the total energy. In case we consider only the first term of the expansion and the cation is located on the *z*-axis we obtain:

$$\Delta E_{POL}^{CL} = -\frac{1}{2}\frac{q^2 \cdot \alpha_{zz}}{R^4} + \cdots \tag{11}$$

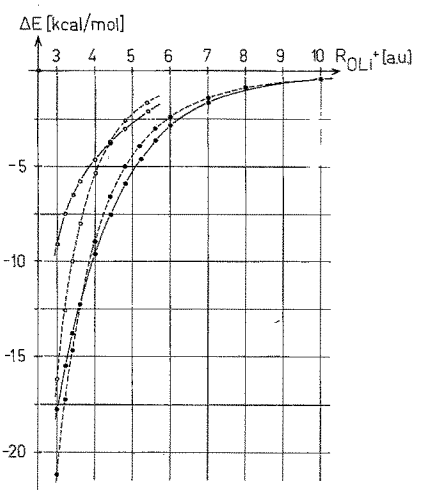

Fig. 8. Comparison of polarization energies calculated with different model assumptions for the complex $Li^+...OH_2$ and $Li^+...OCH_2$.
ΔE_{DEL} in $Li^+...OH_2$ obtained from SCF energy partitioning: —o—o—o—o—.
ΔE_{POL}^{CL} in $Li^+...OH_2$ calculated from Eq.(11): —o——o——o——.
ΔE_{DEL} in $Li^+...OCH_2$ obtained from SCF energy partitioning: —●—●—●—●—●—.
ΔE_{POL}^{CL} in $Li^+...OCH_2$ calculated from Eq.(11): —●——●——●——●—

comparing the results from Eq.(11) with the delocalization energies, ΔE_{DEL} derived from SCF energy partitioning we realize a number of interesting facts (Fig. 8). At the limit of large distances both curves converge asymptotically provided the calculated polarizability has been inserted in Eq.(11). In the medium range there is a systematic underestimation of ΔE_{DEL} by the classical formula which perhaps might be caused by neglect of higher terms in the expansion series (11) called hyperpolarizabilities. Around the energy minimum and at still shorter intermolecular distances we realize an opposite kind of deviation: the values derived from Eq.(11) are substantially larger in absolute value than ΔE_{DEL}.
Formally we can attribute those differences either to another kind of error in the incomplete classical formula (11) or to the presence of other terms in ΔE_{DEL} (5) like the charge transfer term, ΔE_{CHT} and higher order terms. A more detailed energy partitioning according to Morokuma [6] shows indeed that the sum of ΔE_{CHT} and the higher order terms is repulsive at the energy minima of complexes like $Li^+...OH_2$ or $Li^+...OCH_2$ [13, 27]. A more detailed analysis of the validity of the classical formula (11) can be performed only on the basis of a comparison with ΔE_{POL} derived directly from SCF energy partitioning.

Now we come back to the errors we have to expect in the case of SCF calculations with our basis sets. Regarding the experimental data summarized in Table 3 much more accurate results are available for the quadrupole tensor of H_2O than for that of H_2CO. Due to large experimental errors one can expect the most accurately calculated values for θ to be more reliable than the experimental data. In the case of polarizabilities the experimental situation is even worse. The only experimental number available is the average value $\bar{\alpha}$ of H_2O. Therefore the results of the extended SCF calculation coming closest to the experimental value of

$\bar{\alpha}$ [16] seem to represent the most reliable information on α_{zz}. Using experimental values for multipole moments and calculated polarizabilities from the best computations we obtain the following values from Eqs.(10) and (11)

$$(R_{OLi} = 3.4 \text{ a.u.} = 1.80 \text{ Å}):$$
$$Li^+...OH_2: \Delta E^{SC}_{COU} = -39.13 \pm 0.94 \text{ kcal/mole}$$
$$\Delta E^{CL}_{POL} = -19.93 \text{ kcal/mole}$$
$$Li^+...OCH_2: \Delta E^{SC}_{COU} = -31.63 \pm 4.23 \; (-27.85^1) \text{ kcal/mole}$$
$$\Delta E^{CL}_{POL} = -22.67 \text{ kcal/mole}$$

A comparison of these results with the numbers given in Table 8 indicates therefore an error of roughly 15 and 7.5 kcal/mole in the ΔE_{COU} values around the energy minima of $Li^+...OH_2$ and $Li^+...OCH_2$ calculated with basis set *A*. In case of basis set *B* these errors are reduced to 8.5 and 3 kcal/mole respectively. In the total energies of interaction these differences will be compensated in part by the systematic underestimation of ΔE_{POL} due to polarizabilities which appear to be calculated substantially too small [33, 34]. At the present stage of our investigations, however, no reliable estimate concerning the errors in the contribution of electron delocalization can be given on the sole consideration of energy data. A further study of the error compensation at the Hartree-Fock limit will be the subject of a forthcoming analysis [27].

Turning now to the electronic aspects of the delocalization phenomena which accompany complex formation, we shall concentrate the last part of the discussion on an analysis of the wave functions of both complexes. From integrated density curves $\rho(z)$ shown in Figs. 4A and 5A we can see mainly the positions of the nuclei and identify them by different heights of the peaks. Density difference curves $\Delta\rho(z)$ according to Eq.(6) provide much more information: we can realize small changes only in the regions around the Li nucleus and rather drastic changes in the electron distribution of the ligands. In the case of $Li^+...OH_2$ we observe a slight polarization around the Li nucleus. In the region of the ligand, however, we do not find a simple structureless polarization curve but a characteristic pattern most pronounced in the neighborhood of the O nucleus. Electron density is transferred from the H-atoms towards the O atom and even further to the opposite side of the O nucleus. If there is any charge transfer between the subsystem in $Li^+...OH_2$ it appears to be very small. It seemed interesting to see how the polarization pattern of the ligand is formed during an approach of the metal cation along the *z*-axis (Fig. 6). As we can see from these three-dimensional plots, polarization at the Li nucleus falls off much faster with increasing intermolecular distance in comparison to the ligand's polarization pattern. This result reflects the different decrease in the strength of the electrostatic field of an ion and a dipole respectively. Interestingly, the polarization pattern of the ligand remains roughly constant during an approach of the cation. Only the height of peaks changes.

The $Li^+...OCH_2$ system differs from $Li^+...OH_2$ roughly by two features: At comparable intermolecular distances polarization of the H_2CO molecule is

[1] Energy obtained from experimental dipole moment and most accurate calculated value of θ_{zz} (see Table 3).

much more intense and due to the presence of the C nucleus a new peak appears in the polarization pattern which therefore is somewhat more complicated. Secondly, we do not observe an "S" shaped polarization curve in $\Delta\rho(z)$ around the Li nucleus but a small peak indicates the presence of some transfer of electron density from H_2CO to Li^+. Again the change in the integrated density difference function $\Delta\rho(z)$ during an approach of the cation illustrates very well the redistribution of electrons on complex formation (Fig. 7). Since calculations on $Li^+...OCH_2$ have been extended to larger intermolecular distances ($R_{OLi}=10$ a.u.) the fall-off in the polarization pattern can be followed much better in this case. On the whole, both diagrams $\Delta\rho(z)$ of $Li^+...OH_2$ and $Li^+...OCH_2$, demonstrate clearly that the polarization of a molecule in the strong and inhomogenous field of a small cation results in a complex redistribution of electron densities. In general such a process is described only very poorly by the first term of the expansion series in Eq.(11), which corresponds to a homogenous electric field at the limit of vanishing field strength.

In order to learn more details on molecular polarization we decomposed the electron density difference curves in Figs. 4A and 5A into contributions of individual localized molecular orbitals (LMO's). The results are shown in Figs. 4B and 5B. Interestingly all LMO's are polarized in the same direction, towards the Li^+ cation. The shape of all curves is rather similar and can be represented roughly by an "S" shaped curve of the type $y=x\cdot\exp(-x^2)$, which represents the first derivation of a Gaussian lobe. Consequently the complex polarization pattern observed above is not the result of a complicated electron rearrangement in one or more individual LMO's but is brought about by the superposition of these individual contributions. In general *K*-shell electrons are hardly affected by the field of the second molecule or ion and hence do not contribute appreciably to polarization. In case of $Li^+...OH_2$ the major effect results from both lone pair and HO bond electrons. The latter as we can see contribute a little more. Polarization of these kinds of electrons (O lone pairs, HC bonds) is roughly the same in $Li^+...OCH_2$. Due to the larger distance from the cationic center the HC bond electrons are affected somewhat less. The major difference between H_2O and H_2CO, however, is brought about by the presence of mobile π-electrons in the CO bond of the latter molecule. The CO bond electrons contribute much more to molecular polarization than all the other LMO's. The results shown here are more detailed but qualitatively the same as those obtained from the shifts of the centers of LMO's derived from calculations which used a somewhat smaller basis set [2].

Finally, we shall be concerned with charge transfer between subsystems in the complexes $Li^+...OH_2$ and $Li^+...OCH_2$. Perhaps we should emphasize here again that charge transfer is no observable quantity and depends on the model used. The numbers obtained from certain model assumptions are useful therefore only for comparison within a series of different complexes. We calculated the transfer of electron density from the ligand to the metal cation according to the model assumptions Eqs. 7–9 and summarized the results in Table 7. The amount of charge shifted is very small indeed in both examples here. At the energy minimum about 2/1000 of an electron are transferred in $Li^+...OH_2$ and about 13/1000 in

$Li^+...OCH_2$. We can see that the qualitative result inferred from density difference surfaces in Figs. 6 and 7 is reproduced nicely by the numbers of Table 7. Charge transfer is much more important in $Li^+...OCH_2$ than in $Li^+...OH_2$ and falls off very rapidly with increasing intermolecular distance R_{OLi}. Interestingly in our model charge transfer goes through a maximum at distances a little larger than the equilibrium values.

An analysis based on Mulliken populations (Table 6) gives roughly the same picture of polarization and very weak charge transfer from the ligand to the cation. As we have shown already in previous review articles [12, 13] Mulliken populations over-emphasize charge transfer compared to the results derived from our model assumptions. All qualitative features, however, are reproduced nicely.

5. Conclusion

A few final conclusions can be added here. First of all our calculations show that SCF energy partitioning on metal ligand complexes provides a useful tool in analyzing the nature of the interaction and possible sources of errors. The Coulomb energy of interaction is reproduced sufficiently well by the simple expansion series of classical electrostatics. Further investigations are necessary in the case of the contribution of electron delocalization. Polarization energy is one important part of it, but the nature of the other terms is not completely understood now. Within certain limits the errors of calculations using small basis sets or avoiding an explicit consideration of electron correlation can be corrected by using known properties of the isolated subsystems.

An analysis of the complexes' wave functions demonstrates that charge transfer between the subsystems is not important in the kind of examples we have studied here. Mutual polarization of the subsystems leads to a complex pattern of changes in electron densities, which seems to be interpretable in terms of polarization of individual localized molecular orbitals. Further investigation of molecular polarization and polarization energies most probably will provide a better insight into intrinsic errors and limitations of the classical theory of polarization.

An attempt to characterize the nature of the metal-ligand bond in complexes like those investigated here leads to the following conclusion: electrostatic and polarization energies are the driving forces of complex formation. Closed shell repulsion as represented by the exchange contribution represents the most important counteracting force and determines thereby the equilibrium distances. Dispersion energy represents a contribution of probably minor importance only [26–35]. The question of higher order contributions, which seem to be slightly destabilizing around the energy minima, is still open.

Acknowledgements. Dr. A. Beyer kindly supplied us with his calculated values of molecular properties of water and formaldehyde. Two of us (P. S. and W. M.) would like to express their gratitude to the computing centers at the Interfakultäres Rechenzentrum, Universität Wien, and at the Hochschule für Bodenkultur Wien, where part of the computations were performed.

References

1. Kebarle,P.: "Ions and ion-solvent molecule interaction in the gas phase", in: Ions and ion pairs in organic reactions, Szwarc, M. Ed., Vol. 1, pp. 27–83. New York: Wiley Interscience 1972
2. Russegger,P., Schuster,P.: Chem. Phys. Letters **19**, 245 (1973)
3. Pullman,A., Schuster,P.: Chem. Phys. Letters **24**, 472 (1974)
4. Dreyfus,M., Pullman,A.: Theoret. Chim. Acta (Berl.) **19**, 20 (1970)
5. Kollman,P.A., Allen,L.C.: Theoret. Chim. Acta (Berl.) **18**, 399 (1970)
6. Morokuma,K.: J. Chem. Phys. **55**, 1236 (1971)
7. Clementi, E., Davis,D.R.: J. Compt. Phys. **1**, 223 (1966); Veillard,A.: IBMOL Version V (1968)
8. Clementi,E., Popkie,H.: J. Chem. Phys. **57**, 1077 (1972)
9. Rizzi,A., Lischka,H., Schuster,P.: in preparation
10. Mulliken,R.S.: J. Chem. Phys. **23**, 1833, 1841, 2338 and 2343 (1955)
11. Edmiston,C., Ruedenberg,K.: Rev. Mod. Phys. **35**, 451 (1963)
12. Schuster,P.: "Energy surfaces for hydrogen bonded systems", in: The hydrogen bond – recent developments in theory and experiments, Schuster,P., Zundel,G., Sandorfy,C. Eds., Vol 1, in press. Amsterdam: North Holland. 1975
13. Schuster,P., Jakubetz,W., Marius,W.: "Molecular models for the solvation of small ions and polar molecules", in: Topics in current chemistry **60** (1975) in press
14. Dunning jr., Th.H.: J. Chem. Phys. **53**, 2823 (1970)
15. Neumann,D., Moskowitz,J.W.: J. Chem. Phys. **49**, 2056 (1968)
16. Liebmann,S.P., Moskowitz,J.W.: J. Chem. Phys. **54**, 3622 (1971)
17. Arrighini,G.P., Maestro,M., Moccia,R.: Chem. Phys. Letters 1, 242 (1967)
18. Neumann,D., Moskowitz,J.W.: J. Chem. Phys. **50**, 2216 (1968)
19. Salzmann,J.J., Jørgensen,C.K.: Helv. Chim. Acta **51**, 1276 (1968)
20. Nelson jr., R.D., Lude jr., D.R., Maryott,A.A. Eds.: Selected values of dipole moments for molecules in the gas phase. Washington D.C.: Nat. Bureau of Standards 1967
21. Verhoeven,J., Dycmons,A.: J. Chem. Phys. **52**, 3222 (1970)
22. Landolt,H.H., Börnstein,R.: Zahlenwerte und Funktionen, Vol. 1, p. 510. Berlin: Springer-Verlag 1951
23. Huttner,W., Lo,M.-K., Flygare,W.H.: J. Chem. Phys. **48**, 1206 (1968)
24. Diercksen,G.H.F., Kraemer,W.P.: Theoret. Chim. Acta (Berl.) **23**, 387 (1972)
25. Schuster,P., Preuss,H.W.: Chem. Phys. Letters **11**, 35 (1971)
26. Diercksen,G.H.F., Kraemer,W.P., Roos,B.O.: Theoret. Chim. Acta (Berl.) **36**, 249 (1975)
27. Beyer,A., Lischka,H., Schuster,P.: in preparation
28. Morokuma,K., Iwata,S., Lathan,W.A.: "Molecular interactions in ground and excited states" in: The world of quantum chemistry, Daudel,R., Pullman,B. Eds., pp. 277–316. Dordrecht: D. Reidel Publ. Comp. 1974
29. Pullman,A., Armbruster,A.M.: Chem. Phys. Letters (in press)
30. Pullman,A., Berthod,H., Gresh,N.: in preparation
31. Dreyfus,M.: Thèse 3è Cycle, University of Paris 1970
32. Port,G.N.J., Pullman,A.: FEBS Letters **31**, 70 (1973)
33. Lischka,H.: J. Am. Chem. Soc. **96**, 4761 (1974)
34. Lischka,H.: Chem. Phys. **2**, 191 (1973)
35. Kistenmacher,H., Popkie,H., Clementi,E.: J. Chem. Phys. **59**, 5842 (1973)

Dr. A. Pullman
Directeur de Recherches au C.N.R.S.
Institut de Biologie Physico-Chimique
Laboratoire de Biochimie Théorique
associé au C.N.R.S.
13 rue P. et M. Curie
F–75005 Paris, France

Prof. Dr. P. Schuster
Institut für Theoretische Chemie
Universität Wien
Währingerstrasse 17
A-1090 Wien, Austria